REORGANIZATION OF ATMOSPHERIC CIRCULATION BETWEEN 1400-1700 CE AS RECORDED IN A SOUTH POLE ICE CORE

Elena V. Korotkikh[1,2*], Paul A. Mayewski[1,2], Andrei V. Kurbatov[1], Daniel A. Dixon[1], Andrew M. Carleton[3], Kirk A. Maasch[1,2], Jefferson C. Simões[4,1], Michael J. Handley[1], Sharon B. Sneed[1], Douglas Introne[1]

[1] Climate Change Institute, University of Maine, Orono, ME 04469-5790, USA

[2] School of Earth and Climate Sciences, University of Maine, Orono, ME, USA

[3] College of Earth and Mineral Sciences, Department of Geography, Penn State University, University Park, PA, USA

[4] Centro Polar e Climático, Instituto de Geociências, Universidade Federal do Rio Grande do Sul Porto Alegre, RS, Brazil

Corresponding author: Elena V. Korotkikh (elena.korotkikh@maine.edu)

Keywords

Holocene; Present; Paleoclimatology; Antarctica; Ice cores, Little Ice Age, Atmospheric circulation

Abstract

Here we present an ~2000 year high-resolution glaciochemical record from the South Pole. Significant changes in chemical concentrations, accumulation rate, stable water isotopes and deuterium excess records are captured during the period ~1400-1700 CE, indicating a reorganization of atmospheric circulation that occurred in two steps: ~1400-1425 CE and ~1650-1700 CE. Major declines in dust and SO_4^{2-} concentrations are observed ~1400 CE suggesting poleward contraction of the southern circumpolar vortex and potential intensification of westerly air flow, accompanied by a sea ice decrease in the Weddell Sea and potentially also in the Indian sector of the Southern Ocean. The changes in stable water isotopes, deuterium excess, NO_3^- concentration and accumulation rate characterize a second shift in atmospheric reorganization between 1650-1700 CE, reflecting increased marine air mass intrusions and subsequent reduction of the katabatic winds, and a shift to a colder moisture source for South Pole precipitation. These internally consistent changes involving atmospheric circulations and sea ice conditions are also in line with those identified for the recent period, and include associations with the large-scale teleconnections of El Niño Southern Oscillation (ENSO) and the Southern Annular Mode (SAM).

Introduction

A major disturbance of the late Holocene climate is a cooling period in the Northern Hemisphere between ~1400-1850 CE, known as the Little Ice age (LIA) [*Jones and Mann*, 2004; *Matthews and Briffa*, 2005; *Mann et al.*, 2008, 2009; *Wanner et al.*, 2011]. The LIA was most likely driven by a combination of factors including: a decrease in solar output, an increase in volcanic activity and a possible slowdown of the thermohaline circulation [*Mann et al.*, 2009; *Trouet et al.*, 2009; *Wanner et al.*, 2011; *Miller et al.*, 2012]. Several studies report evidence of a climate shift observed during a similar time interval in the Southern Hemisphere (SH) [*Mayewski* *et al.*, 2004a; *Moy et al.*, 2009; *Bertler et al.*, 2011]. Climate changes in the SH are, however, not homogenous, due to the regional differences in environment, climatology and ice dynamics over the vast expanse of Antarctica. A major climate driver in the SH is the Southern Hemisphere Westerlies (SHWs) belt. The intensity and position of the SHWs affect environmental conditions throughout Antarctica [*Mayewski et al.*, 2004b, 2009; *Shulmeister et al.*, 2004; *Bertler et al.*, 2011; *Dixon et al.*, 2012; *Sime et al.*, 2013] Several records from Antarctica and South America suggest a shift in atmospheric circulation and position of the SHWs sometime between 1300-1800 CE, however, they differ in their interpretations of the associated climate conditions and position and strength of the SHWs.

Moy et al. [2009] suggest an intensification and poleward shift of the SHWs and overall colder conditions in southern South America, based on several paleoclimate records from Patagonia. Moreno et al. [2009] show that the SHWs may have achieved their modern state at the beginning of the Little Ice Age, i.e., 570 years ago. Lechleitner et al. [2017] note a pronounced southward shift of the intertropical convergence zone (ITCZ) between 1320-1820 CE. Ceppi et al. [2013] show that the ITCZ tends to shift together with the SHWs, thus a southward shift in ITCZ during the LIA would coincide with a southward shift in the SHWs. Based on ice core records from Siple Dome, Mayewski et al. [2013] suggest a contraction and southward shift of the SHWs and displacement of the Amundsen Sea Low (ASL) closer to coastal West Antarctica ~1600 CE. Kreutz et al. [1997] show an increase in meridional atmospheric circulation intensity in the sub-polar South Pacific at the beginning (~1400 CE) of the LIA. Law Dome records show generally lower temperatures during the period 1350-1800 CE [*Ommen and Morgan*, 1997] . A study from Stenni et al. [2011] reports colder conditions during the LIA in northern Victoria Land, East Antarctica. *Bertler et al.* [2011] published a summary of climatic changes during the LIA (1300-

1800 CE) in Antarctica, suggesting overall cooler conditions during this period, with increased atmospheric circulation, and increased sea ice production in the Ross Sea.

Other proxy records suggest alternate expansion and weakening of the SHWs during the LIA. A study using climate-proxy data from peat bogs reports drier conditions during the LIA in Tierra del Fuego, southern South America, during the LIA which the authors attribute to the equatorward shift of the mean position of the SHWs [*Chambers et al.*, 2014]. Varma et al. [2012], using climate models and marine sediment records from the Chilean continental slope, note that during periods of low solar activity (such as the Maunder Minimum) the SHWs become weaker near Antarctica and the belt expands equatorward. Based on a West Antarctic ice core record, Koffman et al. [2014] suggest that SHWs occupied a more southerly position during the Medieval Climate Anomaly (1050-1400 CE) and shifted northward at ~1430 CE. Meyer and Wagner [2008, 2009], show a northward shift of the SHWs during the LIA, based on both proxy records from South America and climate modeling studies.

Given the somewhat conflicting results of previous studies as to the inferred atmospheric circulation during major climate events such as LIA, in this paper, we present a 2000 year ice core record from the South Pole that shows a shift in several glaciochemical parameters (SO_4^{2-}, NO_3^-, Ti, La, Ce, Pr, $\delta^{18}O$, δD and d-excess) capturing a major reorganization of atmospheric circulation between 1400-1700 CE.

Methodology

2.1 Ice core collection and chemical analysis

An ice core was drilled near South Pole (89.93°S, 144.39°W, elevation of 2808 m a.s.l.) during the 2002/2003 austral summer field season. The core was collected as a "core of opportunity” by Ice Core Drilling Services (ICDS) during construction of the South Pole Remote Earth Science and Seismological Observatory (SPRESSO). The core was subsequently processed by the United States International Trans Antarctic Scientific Expedition team (site US ITASE-02-6).

The section from 0.8 to 200 meters of the South Pole ice core was sampled using the Climate Change Institute continuous melting system at an average sample resolution of ~1 cm. Melted co-registered samples were collected for ICP-SFMS (Inductively Coupled Plasma Sector Field Mass Spectrometry), IC (Ion Chromatography) and stable water isotopes analysis. All samples were analyzed for their major anion (Cl^-, NO_3^-, SO_4^-) content using a Dionex DX-500 ion chromatograph paired to a Gilson Liquid Handler autosampler. Every sample from sections 0.88-59.4 m and 148.9-161 m depth (sample resolution 4-27 samples/year), and every tenth sample from the rest of the core (sample resolution 1-2 samples/year) were analyzed for major and trace elements (Na, Mg, Ca, Sr, Cd, Cs, Ba, La, Ce, Pr, Pb, Bi, U, As, Al, S, Ti, V, Cr, Mn, Fe, Co, Cu, Zn, Li and K) using the Climate Change Institute (CCI) Thermo Electron Element2 ICP-SFMS coupled to a Cetac Model ASX- 260 autosampler. The interferences were minimized by using an ESI Apex desolvating sample introduction system. All samples from the top 6 meters of the core and every 10^{th} sample from the rest of the core were analyzed for stable water hydrogen (δD) and oxygen ($\delta^{18}O$) isotopes. The stable water isotope samples are reported as per mil relative to Standard Mean Ocean Water (SMOW). They were analyzed as vapor on a Picarro Laser Cavity Ringdown Spectrometer (Model L2130-i) with a high throughput vaporizer. The detection limits for major and trace elements, and major ions used in this study (defined as three times the standard deviation of MilliQ (>18.2 MΩ) deonized water blanks passed through the entire continuous melting system) are shown in Table 1.

2.2 Dating of the ice core

The South Pole ice core record was annually dated, using a CCI software package [*Kurbatov et al.*, 2005], by counting seasonal peaks from Na, Sr, S, SO_4^{2-}, and Cl^- (See example in Figure 1a). The timescale was calibrated using major volcanic eruptions, identified by large peaks in S and SO_4^{2-} concentration, as independent age markers (Figure 1b). Ages of volcanic events were adapted from the WAIS Divide timescale [*Sigl et al.*, 2013]. Based on our dating, the South Pole record covers the period from -66 to 1999 CE. The estimated dating error is ±1 year for the period 1963-1999 CE; ±3 years for 1815-1963 CE; ±11 years for 1458-1815 CE; ±12 years for 1257-1458 CE - ±1; and ±24 years for 232-1257 CE. Dating uncertainty before 232 CE is not estimated because of the lack of any known historical eruptions in the deeper section of the core.

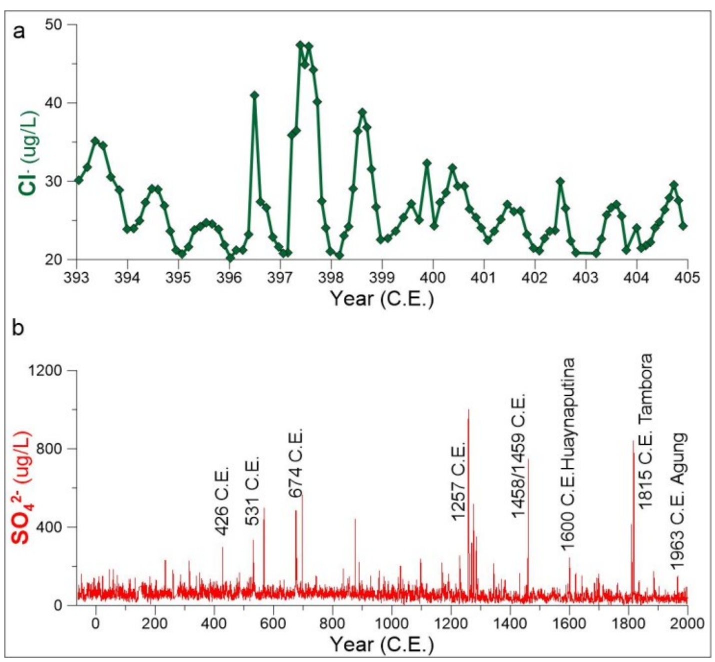

Figure 1. South Pole ice core timescale development. Annual variations in Cl^- (ug/L) concentrations (a) and SO_4^{2-} (ug/L) volcanic record (b).

Table 1. Average method blank concentration (blank), method detection limit (MDL)[1], minimum, maximum and mean sample concentration South Pole ice core used in this study.

			SPRESSO concentrations		
Element	Blank	MDL	Mean	Min	Max
La^{139}(LR) (ng/L)	0.02	0.001	0.37	< MDL	30.36
Ce^{140}(LR) (ng/L)	0.01	0.001	0.77	< MDL	62.26
Pr^{141}(LR) (ng/L)	0.002	0.001	0.09	< MDL	7.08
Ti^{47}(MR) (ng/L)	1.62	3.01	35.48	< MDL	2062.02
NO_3^- (μg/L)	6.73	4.82	84.67	< MDL	197.45
SO_4^{2-} (μg/L)	3.09	0.75	57.60	1.18	1002.89

[1] MDL is defined as three times the standard deviation of 5 MilliQ (>18.2 MΩ) deonized water blanks passed through the entire melter system

LR denotes low-resolution ICP-SMS mode (m/△m=300), and MR denotes medium-resolution mode (m/△m=4000)

The South Pole ice core site and climate influences

The South Pole is located in central Antarctica at an elevation of 2835 m a.s.l. (Figure 2). The prevailing wind direction at the South Pole is from north to east grid, emanating from the high interior of the East Antarctic plateau [*Lazzara et al.*, 2012]. These air masses have low concentrations of aerosols, because of the long distances the particles travel from their sources [*Hogan et al.*, 1982]. The proximity of the South Pole to the lower-altitude West Antarctic ice sheet means that the South Pole region can also be influenced by warmer and more moist air-masses entering West Antarctica from the south-east South Pacific or the south-west South Atlantic Oceans. The South Pole Plateau receives warmer surface air and stronger surface winds than most of the Antarctic interior [*Hogan*, 1997]. Previous studies show that aerosols and particles are usually transported to the South Pole by these warm marine air mass intrusions occurring via the Weddell, Amundsen-Bellingshausen and Ross Seas [*Bodhaine et al.*, 1986; *Shaw*, 1988; *Hogan and Gow*, 1993].

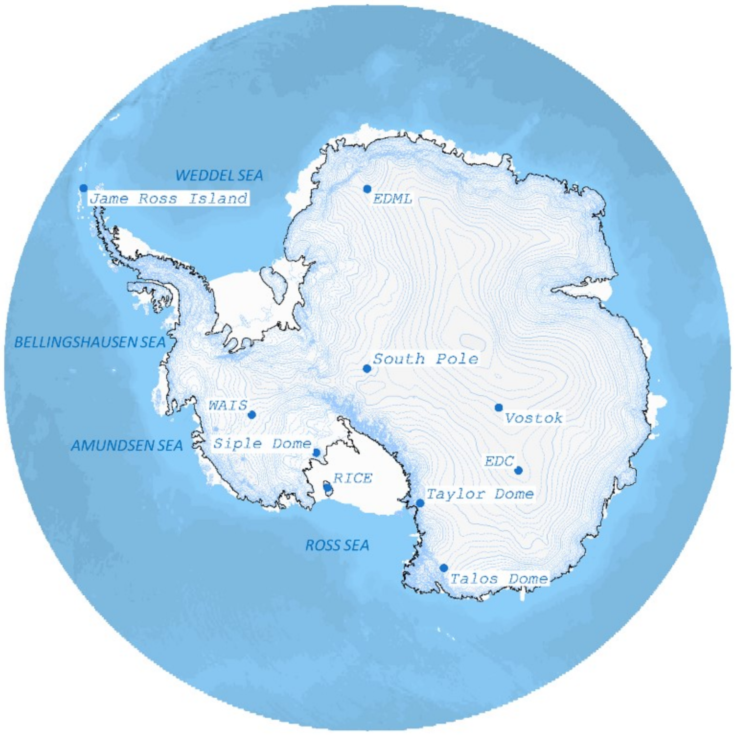

Figure 2. Map of the ice core locations used in this study. (produced using Generic Mapping Tools (GMT) http://gmt.soest.hawaii.edu/).

South Pole glaciochemical records.

A number of glaciochemical records, including stable isotopes, d-excess, SO_4^{2-}, NO_3^-, Ti, La, Ce, Pr, and accumulation rate, were chosen for this study to evaluate climate conditions for the past ~2000 years (Figure 3). Mean values during different time intervals are shown in Table 2.

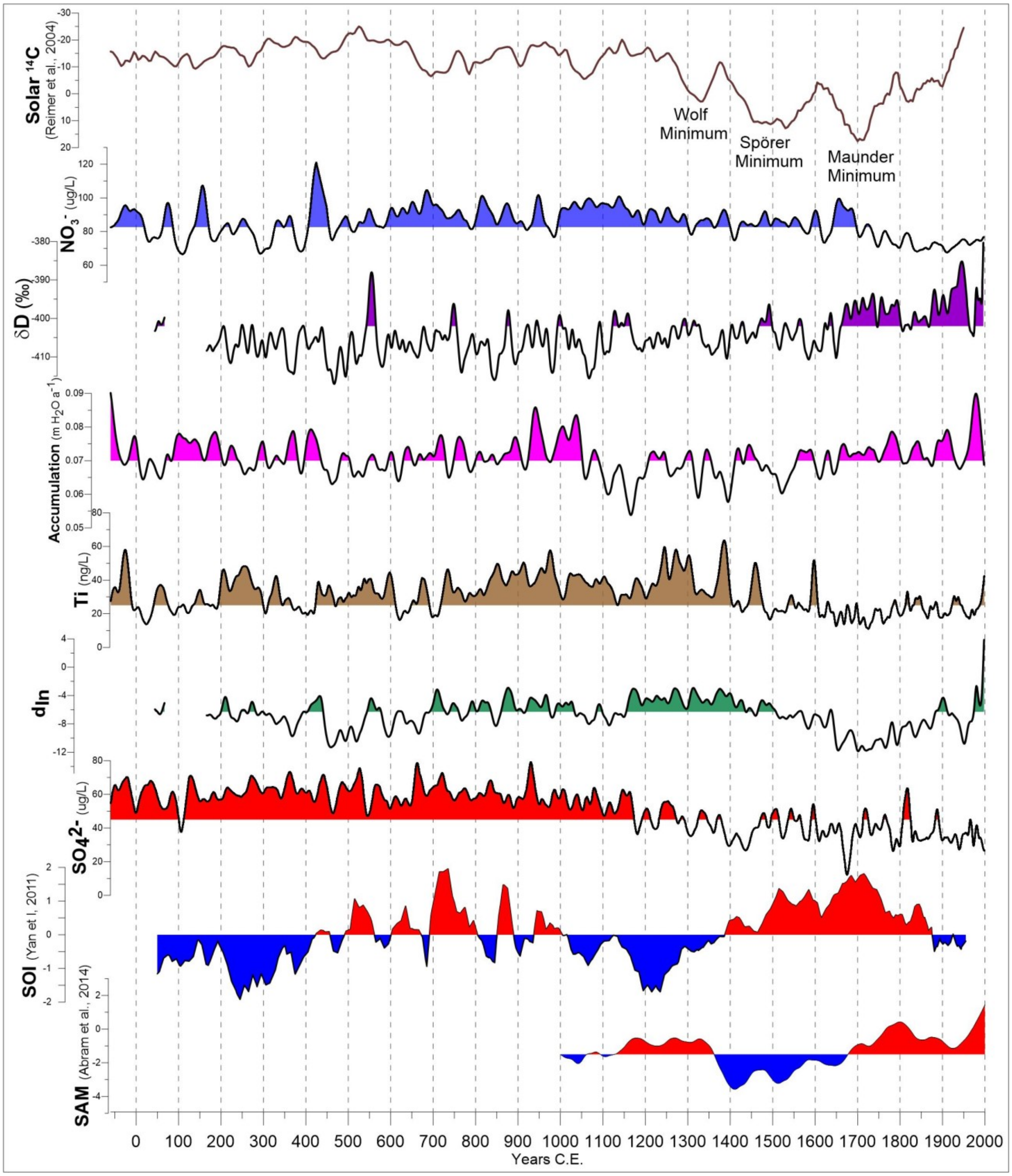

Figure 3. South Pole glaciochemical records: NO_3^- (ug/L), δD (‰), accumulation rate (m H_2O a^{-1}), Ti (ng/L), d_{ln}, and SO_4^{2-}(ug/L). All data shown as a smoothed data estimated using a robust spline smoothing function. Values above the mean are colored for the ice core time series. Also shown are the reconstructed climate indices of the Southern Oscillation (SOI) [*Yan et al.*, 2011], and Southern Annular Mode (SAM) [*Abram et al.*, 2014], and the solar irradiance [*Reimer et al.*, 2004] reconstructions.

Table 2. Mean values of South Pole time series during different periods.

	60 BCE - 400 CE	400 CE - 650 CE	650 CE -1400 CE	1400 CE -1650 CE	1650 CE - 1998 CE
La (ng/L)	0.74	0.34	0.70	0.30	0.31
Ce (ng/L)	1.42	0.61	1.33	0.68	0.70
Pr (ng/L)	0.20	0.07	0.17	0.08	0.07
Ti (ng/L)	54.55	36.49	64.16	37.57	27.66
NO_3^- (ug/L)	81.28	88.01	91.26	83.87	74.05
SO_4^{2-} (ug/L)	63.32	66.52	62.65	46.29	43.52
δO^{18} (‰)	-50.23	-50.33	-50.54	-50.06	-48.72
δD (‰)	-404.69	-406.05	-406.19	-403.47	-393.79
d-excess	-2.82	-3.38	-1.86	-2.97	-4.08

Dust records

The dust signal in the South Pole record is represented by several elements: Ti, La, Ce, and Pr. All elements are highly correlated to each other and have very low crustal enrichment factors when compared to values in Wedepohl [1995], indicating that the primary source for these elements is crustal dust. Figure 3 shows Ti variability for the past ~2000 years (note that other dust elements show similar variability as given in Figure 4). The most elevated dust concentrations are observed until ~1400-1425 CE, except for the ~400-550 CE interval, when some dust elements show a decline in concentration (Table 2). The most significant shift in South Pole dust influx occurs ~1425 CE, when dust element concentrations decrease ~1.5 times.

Dust is transported to the Antarctic from the Southern Hemisphere lower-latitude landmasses via the SHWs. The observed decrease in dust deposition at ~1425 CE suggests changes in strength, latitudinal extent, and dominant pattern (i.e., zonal vs. meridional) of the SHWs. Figure 5 shows that during the period 1958-1998 South Pole Ti is positively correlated with the strength of the zonal near-surface winds. The positive correlation suggests that a decrease in dust concentrations after 1425 CE is related to weakening of the SHWs. A weakening of the SHWs during the LIA is supported by Varma at al. [2012] and suggested to be related to reduced solar irradiance. However, the period for which the correlation in Figure 5 is calculated is not very long. Moreover, one cannot assume that the same relationships between South Pole dust and zonal wind persisted in the past under potentially different climatic conditions. Several studies, in fact, show intensified westerly flow during the LIA [*Kreutz et al.*, 1997; *Shulmeister*, 1999; *Mayewski et al.*, 2004a; *Moy et al.*, 2009; *Bertler et al.*, 2011].

Several studies [*Shulmeister*, 1999; *Mayewski et al.*, 2004a; *Goodwin et al.*, 2012] suggest the dominance of more intense westerly (i.e., zonal) circulation during the LIA and more meridional circulation before the LIA. Under meridional flow conditions, dust could be more easily transported to the South Pole, which would explain the elevated dust levels until ~1425 CE. An increase in zonal flow, conversely, would limit the intrusion of middle-latitude air into the Antarctic interior, potentially causing the decrease in dust concentration noted in the South Pole records during the LIA. Dust deposition at the South Pole is appears to be related to the position of the SHWs. Most of the dust deposited in Antarctica originates from South America and Australia with the southern South American dust source being more significant for the South Pole region [*Li et al.*, 2008; *Neff and Bertler*, 2015]. The most southern major dust sources are in Patagonia (between 38-48ºS), in the region under the influence of the SHWs [*Prospero et al.*, 2002; *Li et al.*, 2008]. Maximum dust activity in Australia is centered on the northeast side of present-day Lake Eyre [*Prospero et al.*, 2002]. Australian dust sources are located farther north, so transport of Australian dust to the South Pole would be more likely during equatorward expansion of the SHWs. Our South Pole dust records suggest that before ~1425 CE the SHWs occupied a more northerly position because concentrations are higher, therefore, involving dust from Patagonia and possibly also Australia. The major decrease in dust deposition ~1425 CE could be a result of the contraction of the SHWs and concomitant poleward shift of the southern circumpolar vortex, thus decreasing exsposure of the dust source areas to SHWs. Several studies, using proxy records from Antarctica, South America and Australia, also suggest a poleward shift of the SHWs during the LIA [*Shulmeister et al.*, 2004; *Moreno et al.*, 2009; *Moy et al.*, 2009; *Mayewski et al.*, 2013]. Other studies, however, argue that SHWs shifted north during the LIA [*Meyer and Wagner*, 2009; *Varma et al.*, 2012; *Chambers et al.*, 2014; *Koffman et al.*, 2015].

Lowered dust concentrations can also be related to changes in precipitation, such that increased precipitation would lead to dust being precipitated out enroute to Antarctica and not reaching South Pole. Our South Pole record does not show any evidence for a precipitation increase at ~1425 CE. However, it does show an increase in accumulation rate and stable water isotopes ~1650 CE, indicating an increase in precipitation that might, at least partially, account for the lower dust levels during the LIA.

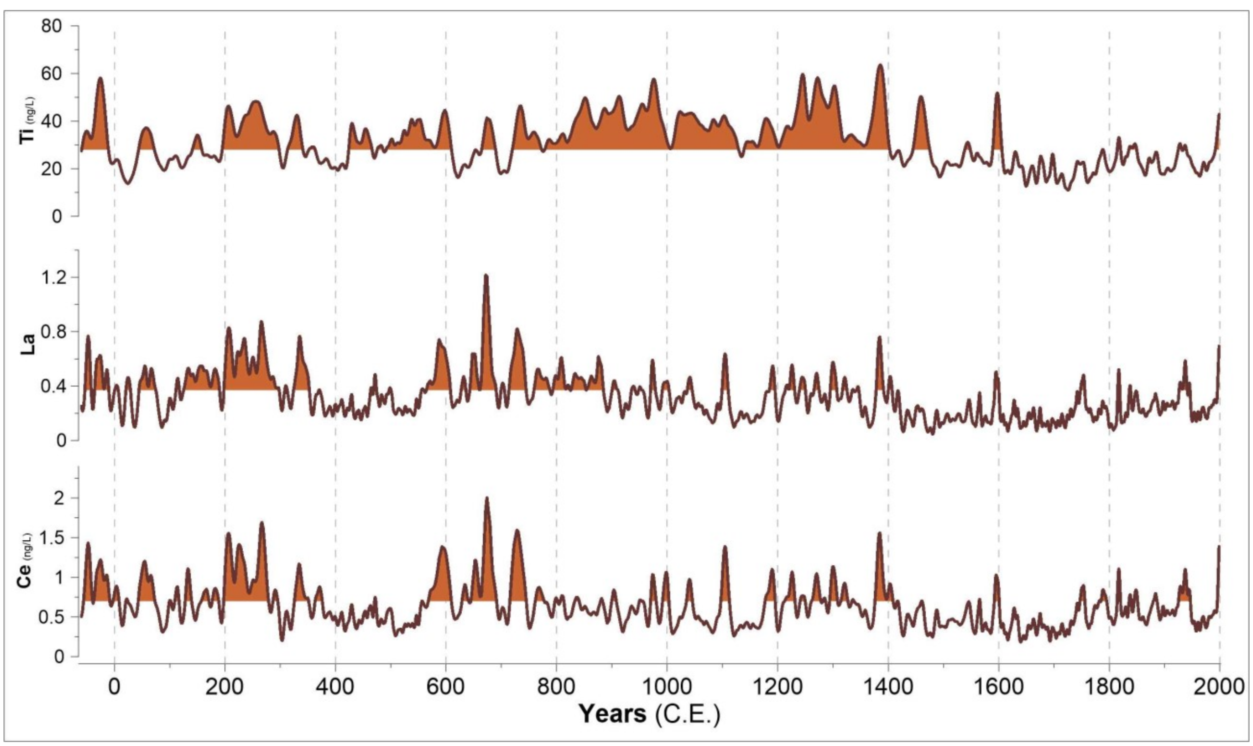

Figure 4. South Pole dust records. Smoothed records of Ti (ng/L), La (ng/L) and Pr (ng/L).

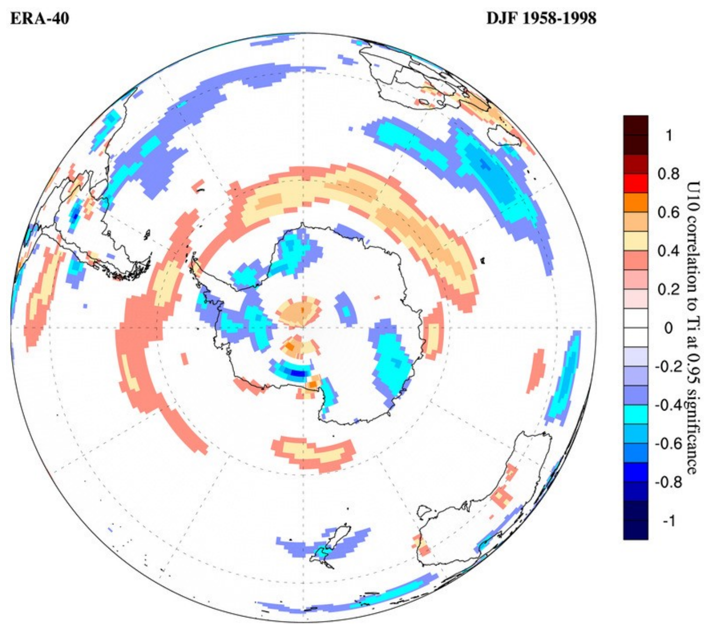

Figure 5. Correlation between South Pole Ti data and surface wind at 10 m (U10) for the period 1958-1998 CE. Correlations were made with the ECMWF 40-year reanalysis (ERA-40) data using Climate Reanalyzer (https://ClimateReanalyzer.org), Climate Change Institute, University of Maine, USA.

SO_4^{2-}

The most elevated SO_4^{2-} values are noted until ~1175 CE, after which time SO_4^{2-} concentration starts to decline. The most pronounced decrease is observed ~1400 CE, shortly preceding the decrease in dust concentrations (Figure 3, table 2).

Except for brief intervals during large volcanic eruptions, the major natural source for SO_4^{2-} in Antarctica is the marine biogenic emission [*Mayewski et al.*, 1990; *Legrand and Mayewski*, 1997]. SO_4^{2-} comes from the oxidation of dimethylsulphide (DMS) produced by marine phytoplankton and emitted from the ocean surface [*Legrand et al.*, 1991; *Minikin et al.*, 1998]. Increased oceanic emission of DMS characterizes glacial intervals due to an increase in sea ice extent [*Welch et al.*, 1993; *Wolff et al.*, 2006].

The South Pole ice core record reveals a decrease in SO_4^{2-} concentrations after ~1400 CE. This could imply a decrease in the production of biogenic sulfate, potentially related to a decrease in sea ice extent or a shift in the atmospheric transport of SO_4^{2-} to interior Antarctica. Variation in snow accumulation may also affect concentrations of sulfate in snow, however, we do not see any correlation between SO_4^{2-} and accumulation in our record. For the period 1979-1998 CE, our South Pole SO_4^{2-} record shows a positive correlation with sea ice extent during austral spring in the Weddell Sea and Indian sectors of the Southern Ocean, and a negative correlation with parts of the Ross Sea (Figure 3.5). Bertler et al. [2011] show an increase in sea ice during the LIA in the Ross Sea. Based on the dipole response of the Ross and Weddell Seas to climate forcing [*Carleton*, 2003; *Lefebvre and Goosse*, 2005] (Figure 6), one would expect a decrease in sea ice during the LIA in the Weddell Sea. We suggest that the decrease in South Pole SO_4^{2-} indicates a decrease in sea ice extent in the Weddell Sea and potentially in the Indian sector of the Southern Ocean since ~1400 CE. A decrease in sea ice extent and therefore a larger amount of open water source is also suggested by changes in South Pole isotopic values discussed below.

The decrease in SO_4^{2-} during the LIA coincides with the major decline in dust concentration, which as discussed earlier could be related to the change to a more zonal atmospheric circulation. Unlike coastal Antarctic sites, South Pole SO_4^{2-} typically shows a maximum sulfate during winter/spring (together with Cl^-), suggesting that biogenic SO_4^{2-} is transported from more distant northerly located areas by winter/spring storms. A decline in SO_4^{2-} concentration since 1400 CE could, therefore, be caused by a contraction of the polar vortex and subsequent decrease in transport of SO_4^{2-} from more distant ocean sources.

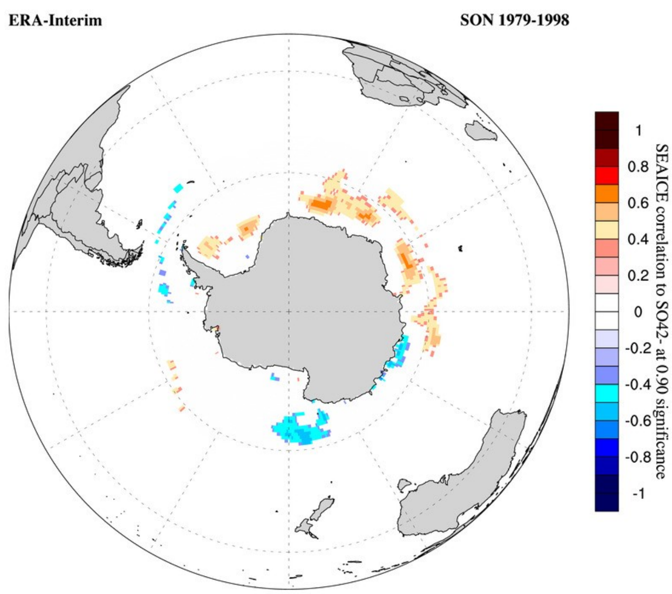

Figure 6. Correlation between South Pole SO_4^{2-} data and sea ice concentration during SON for the period 1979-1998 CE. Correlations were made using European Reanalysis Interim (ERA-Interim) data from Climate Reanalyzer (https://ClimateReanalyzer.org), Climate Change Institute, University of Maine, USA.

Stable water isotopes

The oxygen and hydrogen isotopic composition of polar ice is used to obtain such paleoclimate information as past local surface temperature changes at the precipitation site [*Petit et al.*, 1999]. Our South Pole isotope record shows a weak correlation to the Amundsen-Scott station air temperature (Figure 7). This weak correlation might be attributable to dating uncertainty and/or lack of an annual isotopic signal in the South Pole record. The latter could be explained by the fact that the South Pole ice core was stored in a freezer facility for a few years before it was sampled, and the long storage period might have caused smoothing of the isotopic signal [*Jouzel*, 2003].

Figure 3 shows the δD record for the last ~2000 years. South Pole $\delta^{18}O$ and δD values are relatively stable until ~1650 CE, except for a short-term increase around 550 CE. The timing of the South Pole stable water isotopes increase corresponds to the extreme short-term cooling in the

Northern Hemisphere starting at 536 CE [*Büntgen et al.*, 2016]. Our South Pole record suggests that climate disturbance ~536-550 CE was a global event, which could be caused by an eruption of a tropical volcano [*Dull et al.*, 2019].

A slightly elevated base level is observed for the period 1100-1650 CE compared to earlier times. The most significant shift in water isotopes occurred ~1650 CE, when $\delta^{18}O$ and δD values increased by ~3% compared to the earlier interval. The South Pole record demonstrates that this shift was rapid, occurring in less than a decade.

Stable isotope variability in ice core records is linked to changes in cyclonic activity around Antarctica [*Ekaykin et al.*, 2004]. An increase in cyclonic activity results in more precipitation and higher temperatures as warm air is advected more frequently onto the continent [*Morgan et al.*, 1991; *Ekaykin et al.*, 2004]. Therefore, we interpret the increase in stable isotopes since ~1650 CE as an increase in the penetration of warm marine air masses to the South Pole produced by an increase in cyclonic activity.

Figure 8 shows stable water isotopes from other Antarctic sites revealing the large spatial and temporal climatic variability. Several ice core records show a decrease in stable isotope values during the LIA. Victoria Lower Glacier (VLG) shows cooling between 1300-1800 CE with the transition to colder conditions occurring rapidly, in less than a decade [*Bertler et al.*, 2011]. Talos Dome shows slight cooling since ~1450 CE, accompanied by an increase in accumulation [*Stenni et al.*, 2011]. Taylor Dome reveals cooling between 1400-1800 [*Steig et al.*, 2000]. The WAIS ice core indicates gradual cooling in central West Antarctica during the last 1000 years [*Fudge et al.*, 2013]. EPICA Dome C from East Antarctica indicates cold conditions 1400-1800 CE [*Jouzel et al.*, 2007]. In contrast, several other records show an increase in isotope values during the last few centuries. RICE, in West Antarctica shows warmer conditions since 1450 CE [*RICE community* *members*, 2018]. Located nearby, Siple Dome also suggests warmer conditions [*Brook et al.*, 2005; *Fudge et al.*, 2013]. Records from the Antarctic Peninsula demonstrate warming after ~1700 CE [*Abram et al.*, 2014]. Our records indicate that the South Pole climate is different from other East Antarctic sites, and also from interior of West Antarctica: it shows more similarity with isotopic changes in the Antarctic Peninsula. Thus, South Pole is most likely representing the most interior intrusion of air masses coming from the Weddell and Bellingshausen Seas.

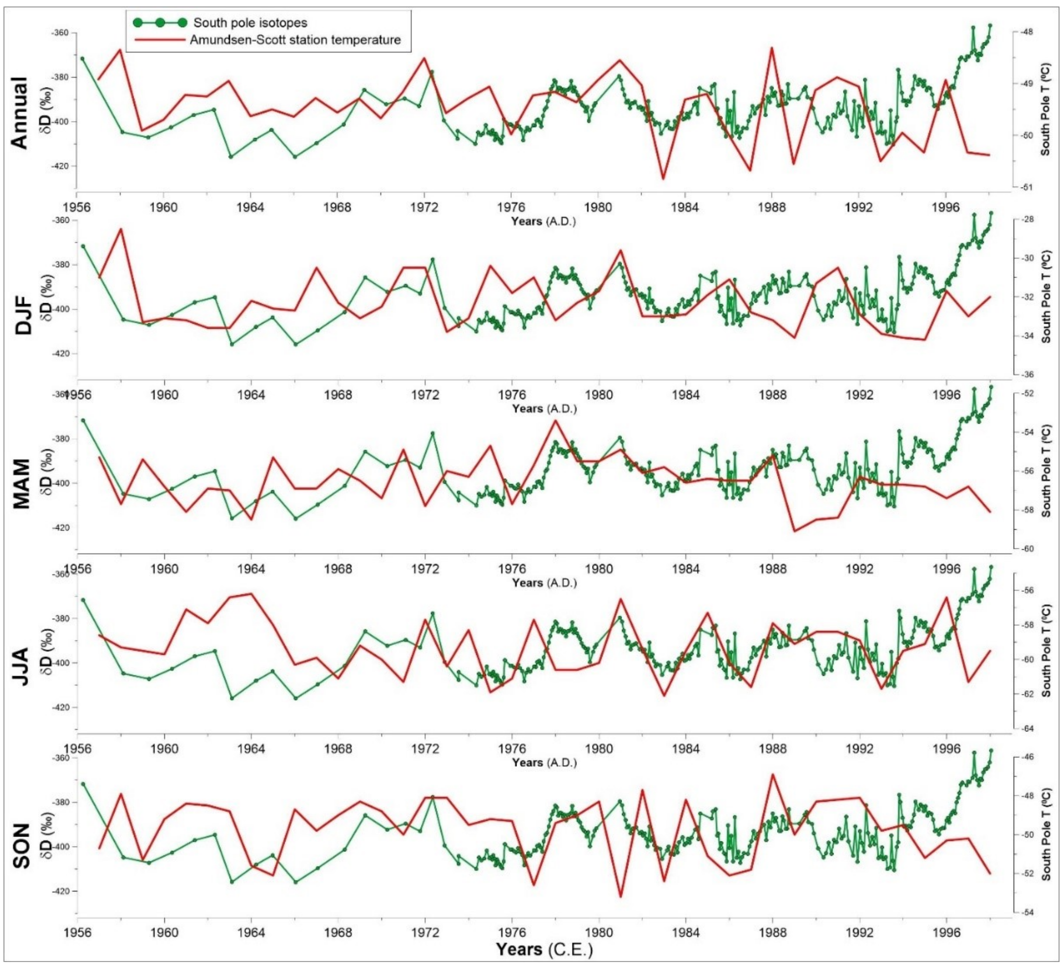

Figure 7. Comparison between South Pole stable water isotopes and Amundsen-Scott temperature records. Amundsen-Scott station temperature records are from https://legacy.bas.ac.uk/met/READER/surface/Amundsen_Scott.00.temperature.html

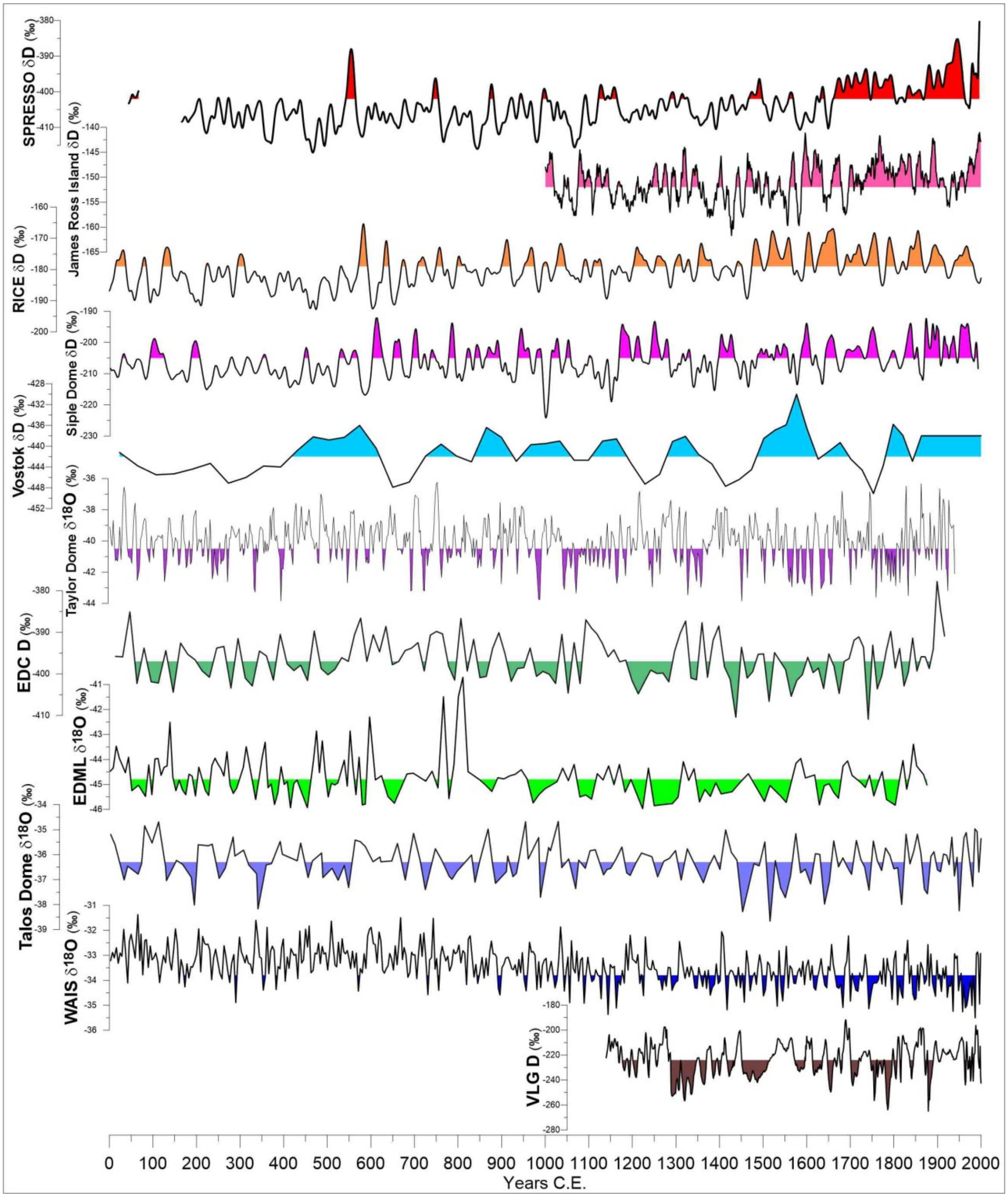

Figure 8. Antarctic stable water isotope records. Stable water isotopes data from top to bottom: South Pole (this study), James Ross Island [*Abram et al.*, 2014], RICE [*RICE community members*, 2018], Siple Dome [*Brook et al.*, 2005; *Fudge et al.*, 2013], Vostok [*Petit et al.*, 1999], Taylor Dome [*Steig et al.*, 2000], EDC [*Jouzel et al.*, 2007], EDML [*Barbante et al.*, 2006], Talos Dome [*Stenni et al.*, 2011], WAIS [*Fudge et al.*, 2013], and VLG [*Bertler et al.*, 2011].

Deuterium excess

Deuterium excess is a second-order isotopic parameter used to assess moisture source [*Vimeux et al.*, 2001]. There are two major factors controlling d-excess: sea surface temperature (SST) during evaporation, and relative humidity at the vapor source region. The d-excess is in general positively correlated with SST, and anticorrelated with relative humidity [*Jouzel et al.*, 2013; *Pfahl and Sodemann*, 2014]. We use the natural log definition of d-excess (d_{ln}) from Uemura at al. [2004]: $d_{ln} = \ln(1+\delta D)-(-2.85\times10^{-2} \times(\ln(1+\delta^{18}O))^2+8.47\times\ln(1+\delta^{18}O))$.

The South Pole mean d_{ln} value is ~ -6.7 ‰ (varying from +7 to -42.7 ‰). Previous studies show that negative d-excess values are observed in ice core sites with elevations lower than 2000 m. The differences in d-excess between low and high elevation sites suggest different moisture source regions, whereby low elevation and coastal locations receive moisture from the colder high-latitude ocean; and interior Antarctic sites having elevations above 2000 m receive moisture from the subtropics and middle latitudes [*Masson-Delmotte et al.*, 2008; *Sodemann and Stohl*, 2009]. The more negative South Pole d-excess values suggest that the South Pole receives precipitation from a more southerly located region than do the more interior areas of East Antarctica.

The d_{ln} at the South Pole (Figure 3) shows that values stay relatively high between 50-1500 CE, except for decrease between ~450-670 CE. The latter d_{ln} deviations, accompanied by lower dust values and short-term increase in stable water isotopes, indicate a climate disturbance similar to the LIA. The highest values are observed between 700 and 1450 CE, indicating warmer SST and lower humidity at the moisture source. The d_{ln} values start to decline after 1450 CE, followed by a sharp decrease at ~1650 CE, suggesting a decrease in SST and increased humidity at the moisture source, or a shift to a colder higher latitude moisture source. Similar to the $\delta^{18}O$ and δD, changes in d_{ln} occur abruptly, over about 10 years, in the South Pole record. The South Pole d_{ln} values reach a minimum at ~1725 CE, then start to rise slowly, except for a sharp drop ~1950 CE.

NO_3^-

The presence of NO_3^- in Antarctic ice cores is attributed to a variety of sources such as tropospheric lightning, NOx produced from N_2O oxidation in the lower stratosphere, galactic cosmic rays and/or surface sources such as biomass burning and NO exhalations from soils [*Legrand and Kirchner*, 1990]. Nitrate concentrations in Antarctic snow are also linked to the extent and/or persistence of polar stratospheric clouds (PSCs) (Mayewski and Legrand, 1990; Mayewski et al., 1995). NO_3^- is transported mostly through the upper troposphere and stratosphere from distant sources [*Legrand and Kirchner*, 1990; *Mayewski et al.*, 2005]. NO_3^- concentration is also assumed to be related to temperature and snow accumulation rate, whereby lower temperatures lead to higher mean NO_3^- concentrations [*Legrand and Mayewski*, 1997] Rothlisberger et al., 2000).

South Pole NO_3^- concentrations exhibit elevated values for the period 60 BCE to ~1700 CE and a decrease from ~1700 CE (Figure 3, Table 2). The decrease in NO_3^-, in general, coincides with a major shift in stable water isotopes, suggestive of increased penetration of marine air masses to the South Pole. More frequent marine air intrusions would, in turn, reduce the katabatic transport of air from the highest locations of the Antarctic interior and subsequently lead to a decrease in deposition of NO_3^- at the South Pole.

Influences of SAM and ENSO teleconnections, and solar activity on South Pole climate variability.

The Southern Annular Mode (SAM) is the dominant pattern of climate and atmospheric variability in the Southern Hemisphere eaxtratropics [*Marshall*, 2003; *Abram et al.*, 2014], and is a measure of the position and strength of the SHWs. Positive SAM is associated with intensification and poleward shift of the SHWs, and low-pressure anomalies over Antarctica compared to middle latitudes [*Swart et al.*, 2015]. Figure 3 shows a SAM reconstruction for the last millennium based on Antarctic temperature proxy records [*Abram et al.*, 2014].

Another major atmospheric circulation driver in the Southern Hemisphere is the tropical El Niño Southern Oscillation (ENSO) [*Carleton*, 2003]. We use an existing proxy-based reconstructions of the Southern Oscillation Index (SOI) for the past 2,000 years [*Yan et al.*, 2011] to capture ENSO variability and changes (Figure 3). The SOI index we use is based on the normalized difference in mean sea level pressure between Tahiti (17.5°S, 149.6°W) and Darwin, Australia, (12.4°S, 130.9°E). Negative SOI anomalies favor El Niño like conditions and positive SOI corresponds to La Niña dominated conditions.

Previous studies demonstrate that polar/tropical teleconnections are stronger when +SAM (-SAM) phases occur with La Niña (El Niño) events, or when ENSO events occur with a weak SAM [*Fogt et al.*, 2011]. The La Niña influence on climate in the SH is very similar to the influence of +SAM. Figure 9 shows the correlation between ENSO (represented by the SOI), SAM and several climate parameters using the ERA-Interim climate reanalysis data. A positive SAM coupled with a La Niña like climate is characterized by deepening of ASL, intensification and poleward contraction of the SHWs, increased precipitation and warming over Antarctic Peninsula and parts of West Antarctica, cooling over most of East Antarctica, decreased sea ice extent in the

Weddell/Bellinsgausen Seas, and increased sea ice in the Ross/Amundsen Seas. The ENSO reconstruction shows La Niña conditions dominated during the LIA, with a more pronounced shift to a negative ENSO ~1600 CE (Figure 3). The SAM reconstruction shows the most negative values ~1400 CE with a positive trend after that (Figure 3).

A number of previous studies show that the South Pole climate is affected by both SAM and ENSO variations [*Meyerson et al.*, 2002; *Lazzara et al.*, 2012]. We compare 25-year resampled South Pole glaciochemical data with SAM and ENSO reconstructions to investigate their long-term associations (Table 3). There is a significant positive correlation between SAM and stable water isotopes, and a significant negative correlation between NO_3^- and d excess (Table 3). An increase in isotopes and decrease in d-excess and NO_3^- concentrations are associated with a trend to more +SAM since ~1650 CE (Figure 3).

Variations in ENSO evidently have a more pronounced influence on South Pole records that the SAM. Table 3 shows a significant negative correlation between SOI and d-excess, SO_4^{2-}, dust, and NO_3^- concentrations; and a positive correlation with stable water isotopes. Decreases in South Pole dust and SO_4^{2-} concentrations coincide with a shift to La Niña dominated conditions ~1400 CE based on the SOI reconstruction. The shift in South Pole water isotopes, accumulation, and NO_3^- records ~1650-1700 CE coincides with maximum in SOI values for that time. However, our South Pole record does not show any major changes during the period 60 BCE to ~1400 CE and suggests relatively stable El- Niño dominated conditions prior to ~1400 CE.

We also investigated the potential influence of changes in solar activity on our South Pole glaciochemical time series. Mayewski et al. [2005] show increased zonal wind strength near the edge of the circumpolar vortex (40-50ºS) during intervals of increased solar activity. Varma et al. [2012], using model output and marine sediment records from the Chilean continental slope, suggest that during periods of low solar activity (Maunder Minimum) the SHWs weaken near Antarctica and expand north, towards the equator. Figure 3 shows a total solar irradiance (TSI) reconstruction based on tree-ring ^{14}C measurements [*Reimer et al.*, 2004]. Table 3 shows that South Pole dust elements, SO_4^{2-} and d-excess are negatively correlated with solar activity, and stable water isotopes are positively correlated. The correlations suggest that during the periods with lower solar activity, like the Maunder Minimum during LIA, South Pole sees a decrease in the dust import, SO_4^{2-} and d excess values, and more positive isotope values.

Table 3. Correlations between 25-year resampled South Pole glaciochemical data and SAM, SOI and solar activity reconstructions. Statistically significant positive/negative correlations ($p<0.1$) are highlighted in yellow/blue. The correlation with the SAM reconstruction [*Abram et al.*, 2014] covers the last ~1000 years, correlations with SOI [*Yan et al.*, 2011] and solar activity reconstruction [*Reimer et al.*, 2004] cover the last ~2000 years.

	SAM	**SOI**	**Solar ^{14}C**
La	0.09	-0.19	-0.29
Ce	0.10	-0.33	-0.30
Pr	0.09	-0.39	-0.32
Ti	-0.09	-0.26	-0.19
NO_3^-	-0.39	0.07	-0.09
SO_4^{2-}	0.17	-0.26	-0.38
$\delta^{18}O$	0.35	0.25	0.27
δD	0.33	0.17	0.23
d_{ln}	-0.32	-0.41	-0.29
Accumulation	0.22	0.14	0.04

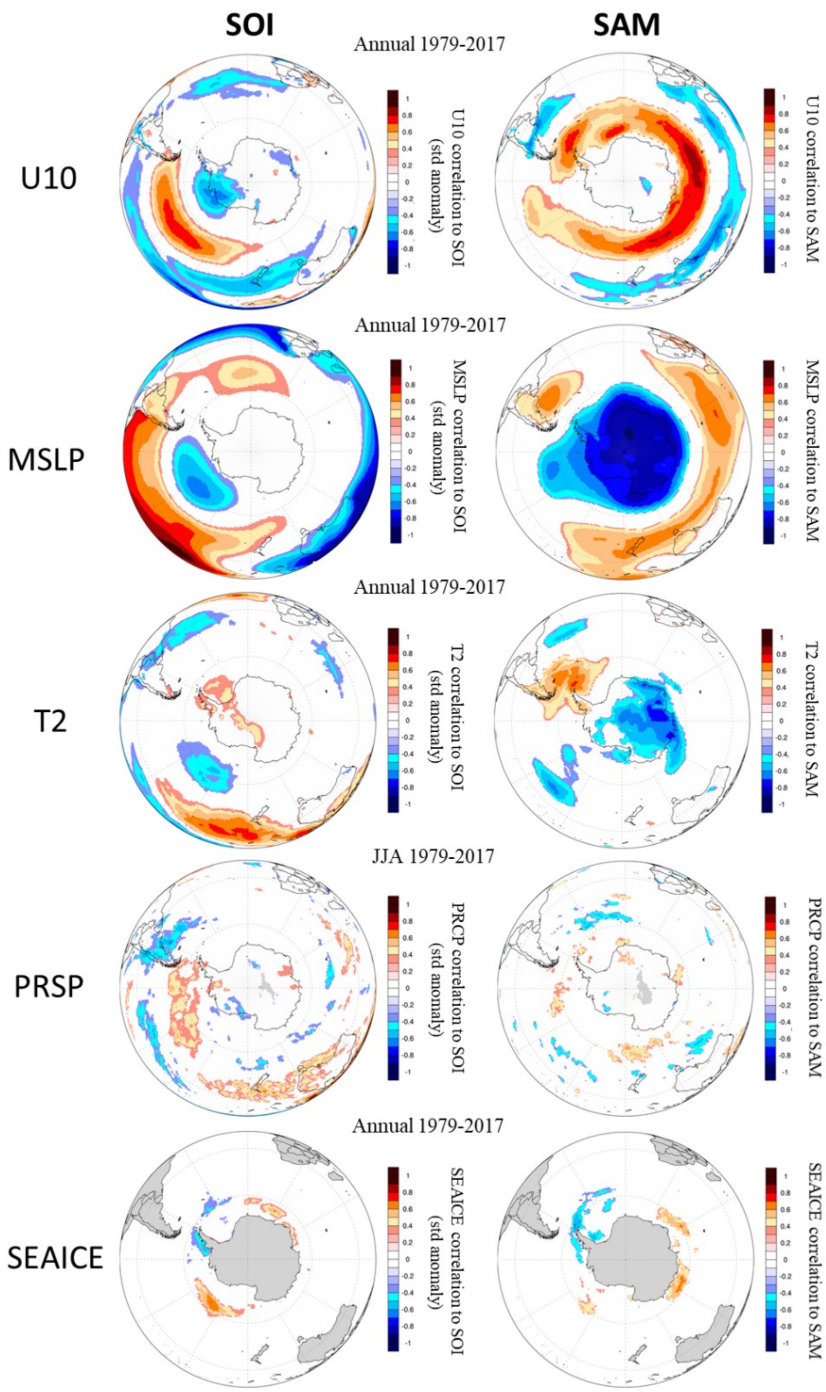

Figure 9. Correlation between SAM, SOI and several surface and near-surface climate parameters. Correlations are shown between SAM and SOI indexes and surface westerly wind at 10 m (U10), mean sea level pressure (MSLP), near-surface temperature (T2), precipitation (PRCP), and sea ice concentration (SEAICE) for the period 1979-2007 CE. Correlations were made using the European Reanalysis Interim (ERA-Interim) data from Climate Reanalyzer (https://ClimateReanalyzer.org), Climate Change Institute, University of Maine, USA. All correlations are at 0.95 significance.

Conclusions

We present an ~2000 year-long high-resolution glaciochemical record from the South Pole. The record reveals major climate changes during the period between 1400-1700 CE, corresponding to the initial and middle stages of the LIA. The most pronounced decrease in SO_4^{2-} is observed ~1400 CE. A significant decrease in dust element concentrations occurs ~1425 CE. The d excess starts to decline after 1450 CE, followed by a sharp decrease at ~1650 CE. South Pole stable water isotopes show a shift to more positive values ~1650 CE, accompanied by an increase in the snow accumulation rate. The NO_3^- record shows a decrease in concentration ~1700 CE. Taken together, the South Pole records demonstrate a major reorganization of atmospheric circulation between ~1400-1700 CE.

Our South Pole glaciochemical record suggests that that atmospheric reorganization occurred in two steps. The first shift in circulation occurred ~1400 CE, as evidenced by a decline in dust and SO_4^{2-}. We suggest that these decreases were the result of a poleward contraction and zonal intensification of the SHWs, thus restricting dust and SO_4^{2-} transport from the middle-latitudes to Antarctica. Changes in SO_4^{2-} also indicate a decrease in winter-spring sea ice extent in the Weddell Sea and in the Indian sector of the Southern Ocean during te LIA, which was countered by an increase in ice extent in the Ross Sea sector.

The second major shift in atmospheric circulation occurred ~1650-1700 CE, as evidenced by major changes in the stable water isotopes, d-excess, and NO_3^- records. This second shift we ascribe to increased cyclonic activity in the sub-Antarctic, with a subsequent enhanced penetration of marine air masses to South Pole, displacement of the moisture source to a colder higher latitude ocean location, reduction of katabatic air transport to the South Pole from the interior of East

Antarctica, and a decrease in sea ice extent in the Weddell Sea. The ~1650-1700 CE atmospheric shift may indicate a further contraction and intensification of the SHWs.

South Pole glaciochemical records show relatively stable climate conditions prior to onset of the LIA, except for the period ~450-650 CE. During the latter interval there is a slight decrease in dust concentration, increase in stable water isotopes and decrease d-excess values, indicative of climate conditions similar to the LIA, but smaller in magnitude. In the Northern Hemisphere, this interval corresponds to a cold event between 400-765 CE, known as the Dark Ages Cold Period [*Wanner et al.*, 2011; *Helama et al.*, 2017] and 536-660 CE Late Antique Little Ice Age [*Büntgen et al.*, 2016].

Correlation of the South Pole ice core record with reconstructions of the SAM and ENSO indices show that both teleconnections have a strong influence on South Pole climatic conditions. In summary, our South Pole glaciochemical records show that prior to ~1400 CE the SH climate was dominated by El Niño-like conditions that changed to a +SAM/La Niña dominated climate conditions during the LIA. These inferences suggest that contemporary associations identified between the indices and their climatic expression operated similarly over the past ~2000 years.

Acknowledgments:

This research was supported by US National Science Foundation Office of Polar Programs grants PRL-1042883, 0439589, 0636506, 0829227, 1203640. We greatly acknowledge the support of the US Antarctic Program, the 109th New York Air National Guard, Ice Coring and Drilling Services, Raytheon Polar Services Company, the National Ice Core Laboratory, Kenn Borek Air Ltd., and our US ITASE field colleagues. We thank Jay Holweger, Bjorn Grigholm and Justin Lambert for assistance with laboratory work.

References:

Abram, N. J., R. Mulvaney, F. Vimeux, S. J. Phipps, J. Turner, and M. H. England (2014), Evolution of the Southern Annular Mode during the past millennium, *Nat. Clim. Chang.*, *4*(7), 564–569, doi:10.1038/nclimate2235.

Barbante, C. et al. (2006), One-to-one coupling of glacial climate variability in Greenland and Antarctica, *Nature*, *444*(7116), 195–198, doi:10.1038/nature05301.

Bertler, N. A. N., P. A. Mayewski, and L. Carter (2011), Cold conditions in Antarctica during the Little Ice Age - Implications for abrupt climate change mechanisms, *Earth Planet. Sci. Lett.*, *308*(1–2), 41–51, doi:10.1016/j.epsl.2011.05.021.

Bodhaine, B. B. A., J. J. Deluisi, J. M. Harris, and G. Monitoringfor (1986), Aerosol measurements at the South Pole, , (January 1977), 223–235, doi:10.1111/j.1600-0889.1986.tb00189.x.

Brook, E. J., J. W. C. White, A. S. M. Schilla, M. L. Bender, B. Barnett, J. P. Severinghaus, K. C. Taylor, R. B. Alley, and E. J. Steig (2005), Timing of millennial-scale climate change at Siple Dome, West Antarctica, during the last glacial period, *Quat. Sci. Rev.*, *24*(12–13), 1333–1343, doi:10.1016/j.quascirev.2005.02.002.

Büntgen, U. et al. (2016), Cooling and societal change during the Late Antique Little Ice Age from 536 to around 660 AD, , *9*(February), doi:10.1038/NGEO2652.

Carleton, A. M. (2003), Atmospheric teleconnections involving the Southern Ocean, *J. Geophys. Res.*, *108*(C4), 8080, doi:10.1029/2000JC000379.

Ceppi, P., Y. T. Hwang, X. Liu, D. M. W. Frierson, and D. L. Hartmann (2013), The relationship between the ITCZ and the Southern Hemispheric eddy-driven jet, *J. Geophys. Res. Atmos.*, *118*(11), 5136–5146, doi:10.1002/jgrd.50461.

Chambers, F. M., S. A. Brain, D. Mauquoy, J. McCarroll, and T. Daley (2014), The 'Little Ice Age' in the Southern Hemisphere in the context of the last 3000 years: Peat-based proxy-climate data from Tierra del Fuego, *Holocene*, *24*(12), 1649–1656, doi:10.1177/0959683614551232.

Dixon, D. a., P. A. Mayewski, I. D. Goodwin, G. J. Marshall, R. Freeman, K. A. Maasch, and S. B. Sneed (2012), An ice-core proxy for northerly air mass incursions into West Antarctica, *Int. J. Climatol.*, *32*(10), 1455–1465, doi:10.1002/joc.2371.

Dull, R. A. et al. (2019), Radiocarbon and geologic evidence reveal Ilopango volcano as source of the colossal ' mystery ' eruption of 539 / 40 CE, *Quat. Sci. Rev.*, *222*, 105855, doi:10.1016/j.quascirev.2019.07.037.

Ekaykin, A. A., V. Y. Lipenkov, I. N. Kuzmina, S. J. Johnsen, and J. R. Petit (2004), The changes in isotope composition and accumulation of snow at Vostok station , East Antarctica , over the past 200 years, , 569–575.

Fogt, R. L., D. H. Bromwich, and K. M. Hines (2011), Understanding the SAM influence on the South Pacific ENSO teleconnection, *Clim. Dyn.*, *36*(7), 1555–1576, doi:10.1007/s00382-010-0905-0.

Fudge, T. J. et al. (2013), Onset of deglacial warming in West Antarctica driven by local orbital forcing, *Nature*, *500*(7463), 440–444, doi:10.1038/nature12376.

Goodwin, I. A. N. D., S. Browning, A. Lorrey, and P. A. Mayewski (2012), A Reconstruction Of The Indo--Pacific Extratropical Atmospheric Longwave Pattern During The Medieval Climate Anomaly IAN D GOODWIN, STUART BROWNING,

Helama, S., P. D. Jones, and K. R. Briffa (2017), Dark Ages Cold Period: A literature review and directions for future research, *Holocene*, *27*(10), 1600–1606, doi:10.1177/0959683617693898.

Hogan, A., S. Barnard, J. Samson, and W. Winters (1982), The transport of heat, water vapor and particulate material to the South Pole Plateau, *J. Geophys. Res.*, *87*(C6), 4287–4292.

Hogan, A. W. (1997), A synthesis of warm air advection to the south polar plateau, *J. Geophys. Res.*, *102*(97), 14009–14020.

Hogan, A. W., and A. J. Gow (1993), Particle transport to the snow surface at the South Pole:the beginning of a troposheric history, , 188–207.

Jones, P. D., and M. E. Mann (2004), Climate over past mellinia, *Rev. Geophys.*, *42*(2003), 1–42, doi:10.1029/2003RG000143.CONTENTS.

Jouzel, J. (2003), Magnitude of isotope/temperature scaling for interpretation of central Antarctic ice cores, *J. Geophys. Res.*, *108*(D12), 4361, doi:10.1029/2002JD002677.

Jouzel, J. et al. (2007), Orbital and millennial antarctic climate variability over the past 800,000 years, *Science (80-.).*, *317*(5839), 793–796, doi:10.1126/science.1141038.

Jouzel, J., G. Delaygue, A. Landais, V. Masson-Delmotte, C. Risi, and F. Vimeux (2013), Water isotopes as tools to document oceanic sources of precipitation, *Water Resour. Res.*, *49*(11), 7469–7486, doi:10.1002/2013WR013508.

Koffman, B., P. Biscaye, S. Goldstein, M. Kaplan, and G. Winckler (2015), Abrupt late Holocene shift in atmospheric circulation recorded by mineral dust in the Siple Dome ice core , Antarctica, , *17*(0), 14504.

Koffman, B. G., K. J. Kreutz, D. J. Breton, E. J. Kane, D. A. Winski, S. D. Birkel, A. V. Kurbatov, and M. J. Handley (2014), Centennial-scale variability of the Southern Hemisphere westerly wind belt in the eastern Pacific over the past two millennia, *Clim. Past*, *10*(3), 1125–1144, doi:10.5194/cp-10-1125-2014.

Kreutz, K. J., P. A. Mayewski, L. D. Meeker, M. S. Twickler, S. I. Whitlow, and I. I. Pittalwala (1997), Bipolar Changes in Atmospheric Circulation During the Little Ice Age, *Science (80-.).*, *277*(August), 1294–1296.

Kurbatov, A. V., P. A. Mayewski, and B. S. Abdul Jawad (2005), Ice Core Dating Software for Interactive Dating of Ice Cores, *Eos, Trans. Am. Geophys. Union. Fall Meet. Suppliment.*, *86*(52), Abstract #PP33C-1603.

Lazzara, M. A., L. M. Keller, T. Markle, and J. Gallagher (2012), Fifty-year Amundsen-Scott South Pole station surface climatology, *Atmos. Res.*, *118*, 240–259, doi:10.1016/j.atmosres.2012.06.027.

Lechleitner, F. A. et al. (2017), Tropical rainfall over the last two millennia: Evidence for a low-latitude hydrologic seesaw, *Sci. Rep.*, *7*(April), 1–9, doi:10.1038/srep45809.

Lefebvre, W., and H. Goosse (2005), Influence of the Southern Annular Mode on the sea ice-ocean system: the role of the thermal and mechanical forcing, *Ocean Sci. Discuss.*, *2*(3), 299–329, doi:10.5194/osd-2-299-2005.

Legrand, M., and S. Kirchner (1990), Legrand and Kirchner : Nitrate in South Polar Precipitation, , *95*, 3493–3507.

Legrand, M., and P. Mayewski (1997), Glaciochemistry of polar ice cores: A review, *Rev. Geophys.*, *35*(3), 219, doi:10.1029/96RG03527.

Legrand, M., C. Feniet-Saigne, E. S. Saltzman, C. Germain, N. I. Barkov, and V. N. Petrov (1991), Ice-core record of oceanic emissions of dimethylsulphide during the last climate cycle, *Nature*, *350*, 144–146.

Li, F., P. Ginoux, and V. Ramaswamy (2008), Distribution, transport, and deposition of mineral dust in the Southern Ocean and Antarctica: Contribution of major sources, *J. Geophys. Res.*

Atmos., *113*(10), 1–15, doi:10.1029/2007JD009190.

Mann, M. E., Z. Zhang, M. K. Hughes, R. S. Bradley, S. K. Miller, S. Rutherford, and F. Ni (2008), Proxy-based reconstructions of hemispheric and global surface temperature variations over the past two millennia, *Proc. Natl. Acad. Sci.*, *105*(36), 13252–13257, doi:10.1073/pnas.0805721105.

Mann, M. E., Z. Zhang, S. Rutherford, R. S. Bradley, M. K. Hughes, D. Shindell, C. Ammann, G. Faluvegi, and F. Ni (2009), Medieval Climate Anomaly, *Science (80-.).*, *326*, 1256–1261.

Marshall, G. J. (2003), Trends in the Southern Annular Mode from observations and reanalyses, *J. Clim.*, *16*(24), 4134–4143, doi:10.1175/1520-0442(2003)016<4134:TITSAM>2.0.CO;2.

Masson-Delmotte, V. et al. (2008), A review of antarctic surface snow isotopic composition: Observations, atmospheric circulation, and isotopic modeling, *J. Clim.*, *21*(13), 3359–3387, doi:10.1175/2007JCLI2139.1.

Matthews, J. A., and K. R. Briffa (2005), The “Little Ice Age”: Re-evaluation of an evolving concept, *Geogr. Ann. Ser. A Phys. Geogr.*, *87*(1), 17–36, doi:10.1111/j.0435-3676.2005.00242.x.

Mayewski, P. a. et al. (2004a), A 700 year record of Southern Hemisphere extratropical climate variability, *Ann. Glaciol.*, *39*(1), 127–131, doi:10.3189/172756404781814249.

Mayewski, P. a. et al. (2004b), Holocene climate variability, *Quat. Res.*, *62*(3), 243–255, doi:10.1016/j.yqres.2004.07.001.

Mayewski, P. A., W. B. Lyons, M. J. Spencer, M. S. Twickler, C. F. Buck, and S. Whitlow (1990), An ice core record of atmospheric response to anthropogenic sulphate and nitrate, *Nature*, *346*(6284), 554–556.

Mayewski, P. A. et al. (2005), Solar forcing of the polar atmosphere, *Ann. Glaciol.*, *41*(1), 147–154, doi:10.3189/172756405781813375.

Mayewski, P. A. et al. (2013), West Antarctica’s sensitivity to natural and human-forced climate change over the Holocene, *J. Quat. Sci.*, *28*(1), 40–48, doi:10.1002/jqs.2593.

Mayewski, P. a et al. (2009), State of the Antarctic and Southern Ocean Climate System (SASOCS), *Rev. Geophys.*, *47*(2007), RG1003, doi: 10.1029/2007RG000231., doi:10.1029/2007RG000231.1.PRELUDE.

Meyer, I., and S. Wagner (2008), The Little Ice Age in southern Patagonia: Comparison between paleoecological reconstructions and downscaled model output of a GCM simulation Three-dimensional radiocarbon modeling: A tool to assess the last glacial ocean circulation and radiocarbon chrono, *PAGES News*, *16*(2), 12–13.

Meyer, I., and S. Wagner (2009), Past Climate Variability in South America and Surrounding Regions, *Paleoenviron. Res.*, *14*, 113–128, doi:10.1007/978-90-481-2672-9.

Meyerson, E. A., P. A. Mayewski, K. J. Kreutz, L. D. Meeker, S. I. Whitlow, and M. S. Twickler (2002), The polar expression of ENSO and sea-ice variability as recorded in a South Pole ice core, *Ann. Glaciol.*, *35*, 430–436, doi:10.3189/172756402781817149.

Miller, G. H. et al. (2012), Abrupt onset of the Little Ice Age triggered by volcanism and sustained by sea-ice / ocean feedbacks, , *39*, 1–5, doi:10.1029/2011GL050168.

Minikin, A., M. Legrand, J. Hall, D. Wagenbach, C. Kleefeld, E. Wolff, E. C. Pasteur, and F. Ducroz (1998), Sulfur-containing species (sulfate and methanesulfonate) in coastal Antarctic aerosol and precipitation, *J. Geophys. Res. Atmos.*, *103*(D9), 10975–10990, doi:10.1029/98jd00249.

Moreno, P. I., J. P. François, R. P. Villa-Martínez, and C. M. Moy (2009), Millennial-scale variability in Southern Hemisphere westerly wind activity over the last 5000 years in SW Patagonia, *Quat. Sci. Rev.*, *28*(1–2), 25–38, doi:10.1016/j.quascirev.2008.10.009.

Morgan, V. I., I. D. Goodwin, D. M. Etheridge, and W. C.W. (1991), Evidence from Antarctic ice cores for recent increases in snow accumulation, *Nature*, *354*(6348), 569–575.

Moy, C. M., P. I. Moreno, R. B. Dunbar, M. R. Kaplan, J. Francois, R. Villalba, and T. Haberzettl (2009), *Past Climate Variability in South America and Surrounding Regions*.

Neff, P. D., and N. A. N. Bertler (2015), Trajectory modeling of modern dust transport to the Southern Ocean and Antarctica, *J. Geophys. Res.*, *120*, 9303–9322, doi:10.1002/2015JD023304.Received.

Ommen, T., and V. I. Morgan (1997), Seasonality in late-Ho;ocene climate from ice-core records, *The Holocene*, *7*(3), 351–354.

Petit, R. J. et al. (1999), Climate and atmospheric history of the past 420,000 years from the Vostok ice core, Antarctica, *Nature*, *399*(6735), 429–413, doi:10.1038/20859.

Pfahl, S., and H. Sodemann (2014), What controls deuterium excess in global precipitation?, *Clim. Past*, *10*(2), 771–781, doi:10.5194/cp-10-771-2014.

Prospero, J. M., P. Ginoux, O. Torres, S. E. Nicholson, and T. E. Gill (2002), Environmental characterization of global sources of atmospheric soil dust identified with the Nimbus 7 Total Ozone Mapping Spectrometer (TOMS) absorbing aerosol product, *Rev. Geophys.*, *40*(1), 1–31, doi:10.1029/2000RG000095.

Reimer, P. J. et al. (2004), IntCal04 terrestrial radiocarbon age calibration, 0-26 cal kyr BP, *Radiocarbon*, doi:10.1017/S0033822200032999.

RICE community members (2018), The Ross Dipole - temperature, snow accumulation, and sea ice variability in the Ross Sea Region, Antarctica, over the past 2700 years, *Clim. Past*, *14*, 193–214, doi:10.5194/cp-14-193-2018.

Shaw, G. E. (1988), Antarctic aerosols: A review, *Rev. Geophys.*, *26*(1), 89–112.

Shulmeister, J. (1999), Australasian evidence for mid-Holocene climate change implies precessional control of Walker Circulation in the Pacific, *Quat. Int.*, *57–58*, 81–91, doi:10.1016/S1040-6182(98)00052-4.

Shulmeister, J. et al. (2004), The Southern Hemisphere westerlies in the Australasian sector over the last glacial cycle: A synthesis, *Quat. Int.*, *118–119*, 23–53, doi:10.1016/S1040-6182(03)00129-0.

Sigl, M. et al. (2013), A new bipolar ice core record of volcanism from WAIS Divide and NEEM and implications for climate forcing of the last 2000 years, *J. Geophys. Res. Atmos.*, *118*(3), 1151–1169, doi:10.1029/2012JD018603.

Sime, L. C., K. E. Kohfeld, C. Le Quéré, E. W. Wolff, A. M. de Boer, R. M. Graham, and L. Bopp (2013), Southern Hemisphere westerly wind changes during the Last Glacial Maximum: Model-data comparison, *Quat. Sci. Rev.*, *64*, 104–120, doi:10.1016/j.quascirev.2012.12.008.

Sodemann, H., and A. Stohl (2009), Asymmetries in the moisture origin of Antarctic precipitation, , *36*(October), 1–5, doi:10.1029/2009GL040242.

Steig, E. J., D. L. Morse, E. D. Waddington, M. Stuiver, P. M. Grootes, P. A. Mayewski, M. S. Twickler, and S. I. Whitlow (2000), Wisconsinan and Holocene Climate History from an Ice Core at Taylor Dome, Western Ross Embayment, Antarctica, *Geogr. Ann. Ser. A Phys. Geogr.*, *82*(2–3), 213–235, doi:10.1111/j.0435-3676.2000.00122.x.

Stenni, B. et al. (2011), Expression of the bipolar see-saw in Antarctic climate records during the last deglaciation, *Nat. Geosci.*, *3*(12), 1–4, doi:10.1038/ngeo1026.

Swart, N. C., J. C. Fyfe, N. Gillett, and G. J. Marshall (2015), Comparing trends in the southern annular mode and surface westerly jet, *J. Clim.*, *28*(22), 8840–8859, doi:10.1175/JCLI-D-15-0334.1.

Trouet, V., J. Esper, N. E. Graham, A. Baker, J. D. Scourse, and D. C. Frank (2009), Persistent positive north atlantic oscillation mode dominated the medieval climate anomaly, *Science (80-.).*, *324*(5923), 78–80, doi:10.1126/science.1166349.

Uemura, R., N. Yoshida, N. Kurita, M. Nakawo, and O. Watanabe (2004), An observation-based method for reconstructing ocean surface changes using a 340,000-year deuterium excess from the Dome Fuji ice core, Antarctica, *Geophys. Res. Lett.*, *31*(13), 2–5, doi:10.1029/2004GL019954.

Varma, V., M. Prange, T. Spangehl, F. Lamy, U. Cubasch, and M. Schulz (2012), Impact of solar-induced stratospheric ozone decline on Southern Hemisphere westerlies during the Late Maunder Minimum, , *39*(October), 1–6, doi:10.1029/2012GL053403.

Vimeux, F., V. Masson, G. Delaygue, J. Jouzel, J. R. Petit, and M. Stievenard (2001), A 420,000 year deuterium excess record from East Antarctica: Information on past changes in the origin of precipitation at Vostok, *J. Geophys. Res.*, *106*(D23), 31863, doi:10.1029/2001JD900076.

Wanner, H., O. Solomina, M. Grosjean, S. P. Ritz, and M. Jetel (2011), Structure and origin of Holocene cold events, *Quat. Sci. Rev.*, *30*(21–22), 3109–3123, doi:10.1016/j.quascirev.2011.07.010.

Wedepohl, K. H. (1995), The composition of the continental crust, *Geochim. Cosmochim. Acta*, *59*(7), 1217–1232.

Welch, K. A., P. A. Mayewski, and S. I. Whitlow (1993), Methanesulfonic acid in coastal antarctic snow related to sea-ice extent., *Geophys. Res. Lett.*, *20*(6), 443–446.

Wolff, E. W. et al. (2006), Southern Ocean sea-ice extent, productivity and iron flux over the past eight glacial cycles., *Nature*, *440*(7083), 491–496, doi:10.1038/nature06271.

Yan, H., L. Sun, Y. Wang, W. Huang, S. Qiu, and C. Yang (2011), A record of the Southern Oscillation Index for the past 2,000 years from precipitation proxies, *Nat. Geosci.*, *4*(9), 611–614, doi:10.1038/ngeo1231.